F. J. WIESNER

Aerodynamic Specialist,
Machinery Advanced
Development Department,
Carrier Air Conditioning Company,
Syracuse, N. Y.
Mem. ASME

A Review of Slip Factors for Centrifugal Impellers

This paper contains a general review of the various methods which have been proposed for the estimation of basic slip factors for centrifugal impellers. As a result of this study, it is concluded that the classical method proposed by Busemann in 1929 is still the most generally applicable prediction for the basic slip factor of centrifugal impellers. The paper then presents a very simple empirical expression, which fits the Busemann results extremely well over the whole range of practical blade angles and number of blades up to a limiting inlet-to-outlet radius ratio for the impeller. An empirical correction factor is also proposed for conditions which exceed this limiting radius ratio. Tabular comparisons of slip factors, with test data (where available), are given for over 60 pump and compressor impellers which have been cited previously in the literature, and the author has added data for several more compressor stages from his own experience.

Introduction

ALTHOUGH much has been written with regard to slip factors for centrifugal impellers, there still seems to be an urgent need to review the various methods which have already been proposed for the calculation of slip factors, and to develop a simple and more universal method for the accurate estimation of slip.

Stodola [1][1] first proposed the now well-known expression for slip velocity in 1927:

$$c_{SL} = \frac{\pi \sin \beta_2}{Z} \cdot u_2 \qquad (1)$$

With relation to the simple impeller discharge velocity diagram shown in Fig. 1:

$$u_2 = c_{u_2}' + \frac{c_{m_2}}{\tan \beta_2} + c_{SL} \qquad (2)$$

or dividing through by u_2 and substituting (1) in (2):

$$1 = \frac{c_{u_2}'}{u_2} + \frac{\phi_2}{\tan \beta_2} + \frac{\pi \sin \beta_2}{Z}$$

or

$$\sigma = \frac{Cu_2'}{u_2} + \frac{Cm_2}{u_2 \tan \beta_2} = \frac{Cu_2'}{u_2} + \frac{\phi_2}{\tan \beta_2}$$
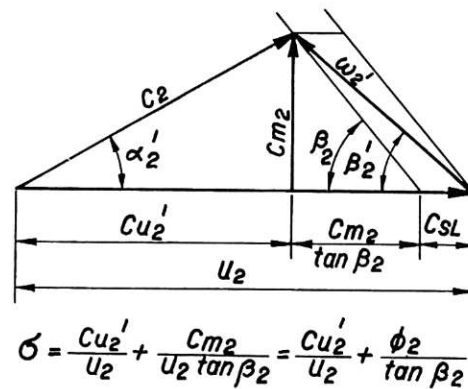
Fig. 1 Impeller discharge velocity diagram

$$\frac{c_{u_2}'}{u_2} + \frac{\phi_2}{\tan \beta_2} = 1 - \frac{\pi \sin \beta_2}{Z} = \sigma \qquad (3)$$

In 1928, Busemann [2] developed what has been termed a more exact theoretical solution which requires rather extensive mathematical treatment. Wislicenus [6] has published curves taken from the original publication, showing Busemann slip factor variations ($\sigma = h_0$) for several discharge blade angles and number of blades. These curves indicate that for a given number of blades (or solidity) and blade angle, there exists a region of relatively constant slip factor and a region of changing slip factor. Wislicenus attempted to define the "solidity" limit which separates these two regions by two different relations:

Nomenclature

c = absolute velocity (or components, when used with subscripts), fps

C_H = impeller tip meridional velocity distribution factor owing to nonuniformity of blade-to-blade flow, dimensionless

l = defined in text

r = impeller radius, in.

u = impeller tip peripheral speed, fps

w = relative velocity, fps

Z = number of blades

α = absolute discharge flow angle, deg

β = impeller discharge blade angle, deg

ϵ_{limit} = impeller radius ratio at limit of "blade solidity"

η = efficiency, expressed in percent/100, dimensionless

λ = impeller tip meridional velocity distribution factor owing to nonuniformity of hub-shroud flow, dimensionless; e.g., Wislicenus' $\pi^2/8$ for sinusoidal velocity profile

μ = head or pressure coefficient, dimensionless

σ = slip factor

ϕ_2 = impeller discharge flow coefficient, dimensionless

ϕ_v = defined in text

Subscripts

m = meridional

SL = slip

u = peripheral

$w\&df$ = windage and disk friction

1 = impeller rms inlet

2 = impeller rms discharge

(Prime values denote flow angles and flow vectors with slip considered)

$$\phi_v = \frac{2\pi}{Z} \qquad (4)$$

and

$$l = \frac{2\pi r_2}{Z} \qquad (5)$$

In 1947, Sheets [7] applied what appears to be an even more adequate expression for these solidity limits (also based on material originally given by Wislicenus), which reduces to:

$$\ln \left(\frac{r_2}{r_1}\right)_{max} \cong \frac{1.30 \cdot 2\pi \sin \beta_2}{Z} \cong \frac{8.16 \sin \beta_2}{Z} \qquad (6)$$

It is the purpose of this paper to show that the Busemann slip factor, applied to the limits of expression (6), is still the most universally accurate method for the estimation of the basic slip factor for centrifugal impellers over the whole range of practical parameters, and that a rather simple empirical expression can be used to calculate essentially the same results. This same expression can also be shown to be in very close agreement with most of the other published slip factor expressions or charts within their implied ranges of applicability. Some of these are as follows:

Stanitz [9], 1952:

$$\sigma = \frac{C_{u_2}'}{u_2} + \frac{\phi_2}{\tan \beta_2} = 1 - \frac{1.98}{Z} \qquad (7)$$

(particularly applicable to straight radial bladed impellers).

Balje [10], 1952, (Fig. 5 of his paper) and also

$$\sigma = \frac{C_{u_2}'}{u_2} \cong \frac{Z}{Z + 6.2(r_1/r_2)^{2/3}} \qquad (8)$$

(for radial bladed impellers only).

Reddy [12], 1954, presented several analytical expressions and a geometrical method, all plotted in Fig. 7 of his paper (also particularly applicable to radial blading).

Kamimoto and Matsuoka [15], 1959, (symbols defined in reference):

$$\sigma = Z \left\{ \left(\frac{\Gamma_Q}{Q}\right) \phi_2 + \frac{1}{2\pi} \left(\frac{\Gamma \omega}{\omega}\right) \right\} \qquad (9)$$

(applied particularly to backward curved impeller blading).

Other methods of estimating slip have been variously published by or attributed to Meisel [3], Pfleiderer [3, 4], Kucharski [3], Sörensen [3, 4], Schulz [3, 4], Yendo [3, 4], Uchimaru [3, 4], Schröder [4], Sheets [7], Emmons [7], Peck [8], Price [8], Anderson [8], Wosika [11], Rogers [21], Maillet and LeManach [21], Acosta [14, 25], and Stahler [24].

Practically, any attempt to determine a slip factor from the input head or work-done factors obtained from test data demands *full* consideration of all of the applicable parameters, which may be arranged as follows:

$$\frac{\mu}{\eta} = \sigma - \frac{C_H \lambda \phi_2}{\tan \beta_2} \pm \mu_1 + \mu_{w\&df} \pm \text{Heat Transfer} \qquad (10)$$

In particular, this shows that there must be accurate knowledge of the effects of tangential (C_H) and cross-channel (λ) velocity profile distortions at the impeller discharge, of the possible presence of inlet prerotation, and of variations of windage and disk friction effects. In addition to these considerations, temperature rise measurements which determine "hydraulic" efficiency must be accurately balanced by the horsepower consumed, and in this, careful attention must therefore be given to all heat transfer effects. In most tests, reconciliation of all of this is no small order, and this is why it has been so difficult to express or derive basic slip factors which ring true enough over the whole range of ap-

plication. A rather large amount of test information is therefore necessary to "average out" these deleterious effects, and to the author's knowledge, this has not been accomplished satisfactorily to date.

Presentation of Data and Empirical Equations

Table 1 includes as many tested pumps and compressors as could be readily obtained in the literature. In addition, this listing contains a representative cross section of compressor stages for which data have not previously been published. Among these stages there are 31 different pumps, ranging from 8.8 to 88 deg in discharge blade angle, and having various blade numbers between 2 and 16. There are also 45 different compressors having discharge blade angles from 20 to 90 deg, with various numbers of blades between 4 and 44. Test information is included for 65 of these stages, 51 of which have been covered in the existing literature. Thirteen of these impellers had actual mean radius ratios which were greater than the calculated "limiting" mean radius ratios using equation (6). These will be dealt with separately in the discussions to follow.

In order to utilize the available test information, it was assumed that heat transfer, prerotation, and cross-channel velocity profile distortions were negligible. A "slip coefficient" was then defined as:

$$\left[\frac{\mu}{\eta} + \frac{C_H \phi_2}{\tan \beta_2}\right] = \sigma \left[1 + \frac{\mu_{w\&df}}{\sigma}\right] \qquad (11)$$

At peak efficiency it is common to find that the value of $\mu_{w\&df}/\sigma$ is quite small and would fall within the error band of test data. Thus a comparison can be made between the values of slip coefficient as obtained from test data at the point of best efficiency, and the corresponding values of slip factor obtained through the use of the various defining equations.

In general, the test slip coefficients contained in Table 1 can be seen to correlate very well with the basic slip factors as specified by Busemann, and it has been found that these, in turn, can be very closely expressed by the simple empirical function:

$$\sigma = 1 - \frac{\sqrt{\sin \beta_2}}{Z^{0.70}} \qquad (12)$$

which is taken to be applicable up to the limit of blade solidity based on equation (6):

$$\epsilon_{limit} = \frac{r_1}{r_2} \cong \frac{1}{\ln^{-1} \dfrac{8.16 \sin \beta_2}{Z}} \qquad (13)$$

For impeller mean radius ratios in excess of this limit, the following equation has been found to be in fair agreement with the Busemann (h_0) results in these areas:

$$\sigma = \left(1 - \frac{\sqrt{\sin \beta_2}}{Z^{0.70}}\right) \left[1 - \left(\frac{\dfrac{r_1}{r_2} - \epsilon_{limit}}{1 - \epsilon_{limit}}\right)^3\right] \qquad (14)$$

Fig. 2 demonstrates the results of these equations in comparison with the Busemann h_0-curves published by Wislicenus. Table 1 contains the various important dimensions and parameters for each particular impeller, as well as the results of equations (12) or (14), and (13) in each case. Also included are the corresponding Busemann, Stodola, and Stanitz slip factors, test values of the flow coefficients ϕ_2 at best efficiency, and the related test values of the slip coefficient $\left(\dfrac{\mu}{\eta} + \dfrac{C_H \phi_2}{\tan \beta_2}\right)$ for each stage. In the latter representation, C_H was taken from Wislicenus [6], Fig. 54. Actually, this was a significant correction only for those stages where the impeller mean radius ratios exceeded the limits of equation (13).

Fig. 3 shows a plot of all of the test values for slip coefficient

KEY : BUSEMANN———————; EMPIRICAL ———————
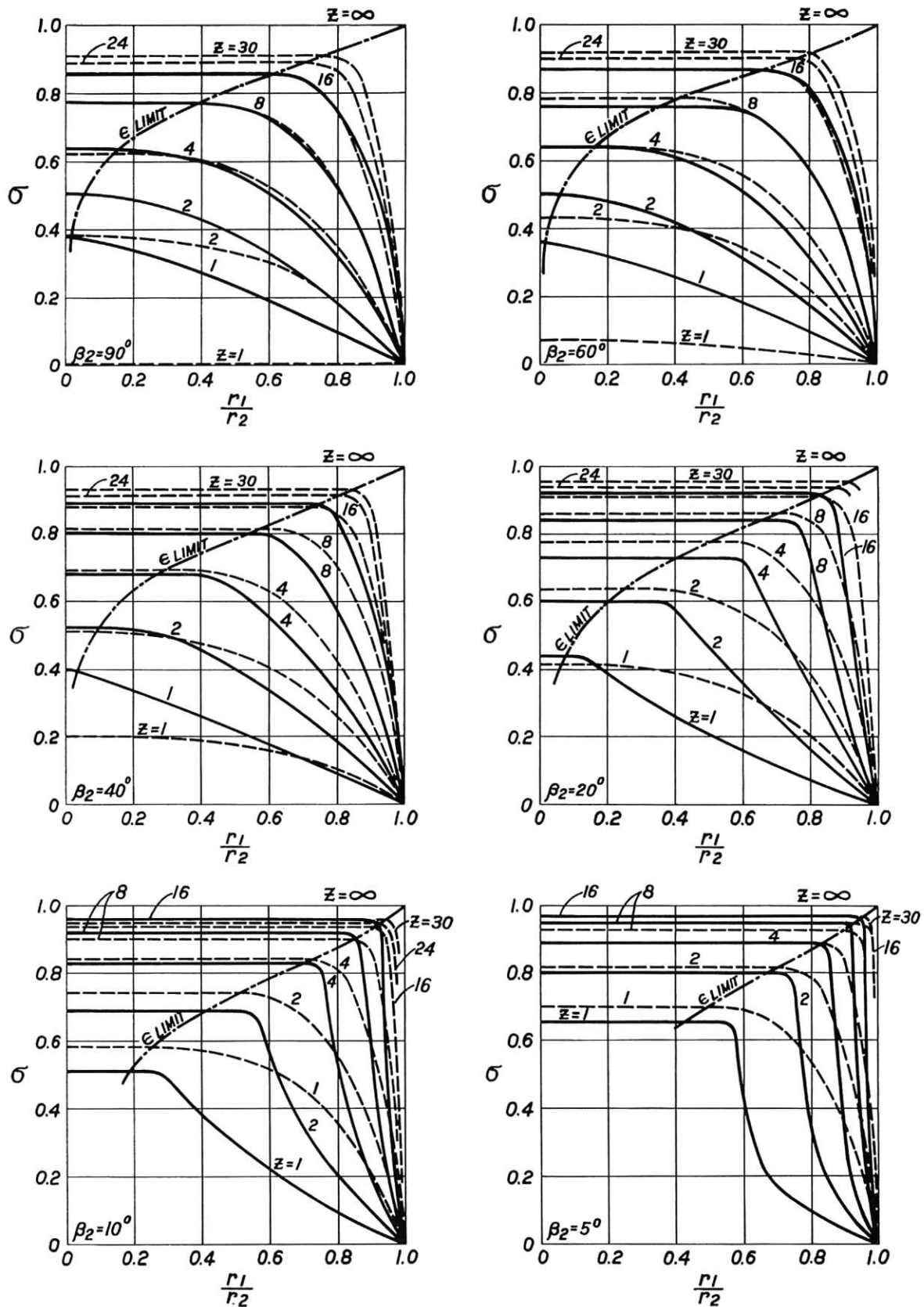
EMPIRICAL EQUATIONS

$$\sigma = 1 - \frac{\sqrt{\sin \beta_2}}{z^{0.70}} \ \text{UP TO} \ \epsilon_{LIMIT} = \frac{1}{\ln^{-1} \frac{8.16 \sin \beta_2}{z}} \ , \text{THEREAFTER} \ \sigma = \left(1 - \frac{\sqrt{\sin \beta_2}}{z^{0.70}}\right)\left[1 - \left(\frac{\frac{r_1}{r_2} - \epsilon_{LIMIT}}{1 - \epsilon_{LIMIT}}\right)^3\right]$$

Fig. 2 Comparison between Busemann and empirical slip factors

Table 1 Calculated and experimental slip factors for centrifugal impellers

Source	Reference	Stage Designation	Pump or Compr.	Mixed or Radial Flow	Mean Impeller Diameter, Inches	β_2 Degrees	Z Number of Blades	Mean Radius Ratio	ϵ_{LIMIT}	$1 - \dfrac{\sqrt{\sin \beta_2}}{Z^{0.70}}$	Busemann σ **	Stodola σ	Stanitz σ	σ of Reference	Flow Coefficient ϕ_1 @ Peak Eff.	Test "Slip Coefficient" $\dfrac{\mu}{\eta} + \dfrac{C_u \phi_2}{\tan \beta_2}$
Wood, Et al	25	R1-7A	P	MF	6.52	8.8	3	0.533	0.659	0.818	0.795	0.840	0.845	0.845	0.100	0.864 (min)
Wood, Et al	25	R1-2AX	P	MF	6.64	9.1	3	0.523	0.724	0.849	0.830	0.876	0.505	0.850	0.057	0.824
Varley	19	Impeller 8	P	RF	9.60	15.4	5	0.338	0.655	0.835	0.803	0.838	0.604		0.090	0.786 (max)
Wood, Et al	25	R1-15A	P	RF	5.44	15.4	6	0.463	0.696	0.852	0.828	0.861	0.670	0.810	0.100	0.832
Acosta, Et al	11	3 Dimensional	P	RF	12.875	17.0	5	0.420	0.620	0.824	0.788	0.817	0.604	0.800		
Peck	8	Impeller A	P	RF	10.00	20.0	6	0.600	0.628	0.833	0.800	0.821	0.670		0.125	0.774
Peck	8	Impeller B	P	RF	10.75	20.0	6	0.558	0.628	0.833	0.800	0.821	0.670		0.169	0.868
Kasai	4	Impeller 7	P	RF	10.00	20.0	7	0.535	0.671	0.850	0.824	0.847	0.717		0.120	0.925
Wiesner	16	Figure 1	C	RF	19.50	20.0	8	0.479	0.705	0.863	0.845	0.866	0.753			
Acosta, Et al	11	Impellers A & B	P	RF	10.30	23.5	6	0.583	0.581	0.819*	0.787	0.791	0.670		0.100	0.792*
Wood, Et al	25	R1-6A	P	MF	6.44	25.5	4	0.540	0.415	0.743*	0.692	0.660	0.505	0.760	0.200	0.721*
Wood, Et al	25	R1-5A	P	MF	6.44	25.5	5	0.540	0.495	0.786*	0.745	0.730	0.604	0.800	0.210	0.768*
Wood, Et al	25	R1-1	P	MF	6.44	25.5	6	0.540	0.556	0.812	0.772	0.775	0.670	0.825	0.200	0.829
Kasai	4	Impeller 6	P	RF	10.00	26.0	7	0.535	0.599	0.830	0.802	0.803	0.717		0.198	0.838
Varley	19	Impeller 7	P	RF	9.60	27.0	2	0.338	0.156	0.579*	0.552	0.288	0.010		0.047	0.610*
Varley	19	Impeller 6	P	RF	9.60	27.0	3	0.338	0.290	0.687*	0.635	0.525	0.340		0.050	0.675*
Varley	19	Impeller 5	P	RF	9.60	27.0	4	0.338	0.396	0.744	0.698	0.644	0.505		0.052	0.725
Varley	19	Impeller 1	P	RF	9.60	27.0	5	0.338	0.476	0.781	0.740	0.715	0.604		0.057	0.765
Varley	19	Impeller 2	P	RF	9.60	27.0	6	0.338	0.539	0.807	0.776	0.763	0.670		0.058	0.826
Varley	19	Impeller 3	P	RF	9.60	27.0	8	0.338	0.629	0.842	0.822	0.822	0.753		0.057	0.910
Varley	19	Impeller 4	P	RF	9.60	27.0	12	0.338	0.734	0.881	0.872	0.881	0.835		0.060	0.975
Kaminoto, Et al	15	Log Spiral	P	RF	200 mm	30.0	6	0.600	0.506	0.792*	0.752	0.738	0.670	0.735	0.200	0.674*
Kasai	4	Impeller 8	P	RF	10.00	30.0	7	0.535	0.558	0.818	0.795	0.776	0.717		0.172	0.785
Sheets	7	Backward-Curved	PorC	RF		30.0	11	0.330	0.690	0.868	0.860	0.857	0.820	0.863	~.180	~.800
Peck	8	Impeller C	P	RF	10.00	32.0	16	0.600	0.763	0.895	0.897	0.896	0.877			
Kaminoto, Et al	15	Circular Arc	P	RF	200 mm	35.0	6	0.600	0.458	0.769*	0.735	0.700	0.670	0.735	0.175	0.647*
Wiesner	16	Figure 2	C	RF	19.50	35.0	18	0.544	0.771	0.899	0.907	0.900	0.890		0.190	0.897

* Includes Radius Ratio Correction & C_H Correction
** Per Wislicenus for up to 16 blades, extrapolated beyond 16 blades
*** Probably less than ϵ_{LIMIT}

Table 1 (continued)

Source	Reference	Stage Designation	Pump of Compr.	Mixed or Radial Flow	Mean Impeller Diameter, Inches	β_2 Degrees	Z, Number of Blades	Mean Radius Ratio	ϵ_{LIMIT}	$\sigma = 1-\dfrac{\sqrt{\sin\beta_2}}{Z^{0.7}}$	Busemann σ **	Stodola σ	Stanitz σ	σ of Reference	Flow Coefficient ϕ_2 @ Peak Eff.	Test "Slip Coefficient" $\dfrac{\mu}{\eta}+\dfrac{C_H\,\phi_2}{\tan\beta_2}$
Kearton	3	4 Bladed	C	RF	15.00	40.0	4	0.566	0.269	0.649*	0.590	0.495	0.505		0.191	0.602*
Varley	19	Impeller 9	P	RF	9.60	40.0	5	0.338	0.350	0.740	0.710	0.596	0.604		0.058	0.750
Kasai	4	Impeller 9	P	RF	10.00	40.0	7	0.535	0.472	0.793*	0.760	0.711	0.717		0.189	0.813*
Kearton	3	6 Bladed	C	RF	15.00	40.0	6	0.566	0.519	0.812	0.800	0.748	0.753		0.190	0.792
Kearton	3	16 Bladed	C	RF	15.00	40.0	16	0.566	0.720	0.884	0.899	0.874	0.876		0.185	0.873
Kearton	3	32 Bladed	C	RF	15.00	40.0	32	0.566	0.848	0.929	0.940	0.937	0.938		0.183	0.963
Dallenbach	20	GTC 85-20-30 #2	C	RF		41.4	11	***	0.680	0.871	0.870	0.852	0.859	0.800		
Stanitz	9	Tan-1 (-1.0)	C	RF		45.0	20	0.490	0.749	0.896	0.906	0.889	0.901	0.904		
Kasai	4	DM B Impellers	C	RF	23.62	47.5	17	***	0.701	0.881	0.889	0.864	0.884		0.223	0.874
Wiesner	16	Impeller 10	P	RF	10.00	50.0	7	0.535	0.499	0.768**	0.750	0.656	0.717		0.186	0.799**
		Figure 3	C	RF	7.50	50.0	16	0.343	0.676	0.874	0.877	0.850	0.876		0.310	0.910
		DM 4A	C	RF	20.47	50.0	19	0.531	0.719	0.888	0.898	0.874	0.896		0.238	0.870
Dallenbach	20	GTP 30	C	RF		53.4	15	***	0.646	0.865	0.865	0.832	0.868	0.840		
Dallenbach	20	GTC 85-30 #1	C	RF		54.5	13	***	0.599	0.850	0.846	0.803	0.818	0.860		
	20	GTC 85-20 #1	C	RF		54.9	14	***	0.620	0.857	0.855	0.816	0.858	0.800		
		400A	C	RF	22.00	55.0	19	0.519	0.703	0.884	0.894	0.865	0.896		0.350	0.886
		DM 2A & 3A	C	RF	25.67	55.0	19	0.524	0.703	0.884	0.894	0.865	0.896		0.268	0.874
		400C	C	RF	22.00	55.0	21	0.475	0.727	0.892	0.902	0.878	0.906		0.350	0.887
Wiesner	16	Figure 15	C	RF	34.00	57.0	18	0.358	0.683	0.878	0.889	0.854	0.890		0.310	0.912
Wiesner	16	Figure 4	C	RF	8.00	57.5	13	0.441	0.588	0.847	0.843	0.796	0.848		0.280	0.869
Varley	19	Impeller 10 #1	P	RF	9.60	59.0	5	0.338	0.246	0.698**	0.671	0.463	0.604		0.059	0.794**
Dallenbach	20	GTCP-105 #1	C	RF			17	***	0.662	0.872	0.870	0.842	0.884	0.871		
		350CA	C	RF	16.50	60.2	19	0.575	0.688	0.881	0.890	0.857	0.896		0.305	0.910
Stanitz	9	Tan-1 (-0.5)	C	RF		63.4	20	0.490	0.694	0.883	0.892	0.860	0.901	0.901		
Dallenbach	20	GTCP-105 #2	C	RF		63.6	15	***	0.614	0.856	0.858	0.813	0.868	0.830		
Wiesner	16	Figure 6	C	RF	10.50	64.2	16	0.548	0.631	0.863	0.868	0.823	0.877		0.355	0.879
Wiesner	16	Figure 6	C	RF	29.75	65.7	18	0.383	0.661	0.873	0.884	0.841	0.890		0.250	0.878
Dallenbach	20	GTCP-185-1	C	RF	13.90	67.0	18	***	0.658	0.873	0.883	0.840	0.890	0.864		
		Impeller U	C	RF	4.67	68.0	11	0.417	0.502	0.820	0.811	0.736	0.820		0.285	0.815
		C8-50	C	RF	38.00	68.0	18	0.445	0.656	0.872	0.884	0.839	0.890		0.325	0.841
Wood, Et al	25	R1-4A	P	MF	6.66	69.3	16	0.523	0.620	0.861	0.860	0.816	0.877	0.900	0.155	0.832

* Includes Radius Ratio Correction & C_H Correction
** Per Wislicenus, for up to 16 blades, extrapolated beyond 16 blades
*** Probably less than ϵ_{LIMIT}

Table 1 (continued)

Source	Reference	Stage Designation	Pump or Compr.	Mixed or Radial Flow	Mean Impeller Diameter, Inches	β_2 Degrees	Z, Number of Blades	Mean Radius Ratio	ε_{LIMIT}	$\sigma = 1-\frac{\sqrt{\sin\beta_2}}{Z^{0.70}}$	Busemann σ **	Stodola σ	Stanitz σ	σ of Reference	Flow Coefficient ϕ_2 @ Peak Eff.	Test "Slip Coefficient" $\frac{\mu}{\eta}+\frac{C_H\,\phi_2}{\tan\beta_2}$
Varley	19	Impeller 11	P	RF	9.60	74.0	5	0.336	0.208	0.679*	0.665	0.396	0.604		0.060	0.824*
		D2 – Hi Flo	C	RF	15.75	75.0	17	0.453	0.628	0.864	0.872	0.822	0.884		0.310	0.891
Kramer, Et al	17	MFI-1A	C	MF	4.40	84.0	14	0.493	0.831	0.929	0.950	0.929	0.955			0.932
Dallenbach	20	MFI-I, IB & O	C	MF	8.82	84.5	17	0.532	0.620	0.862	0.867	0.816	0.884	0.810		0.862 ??
Dallenbach	20	MFI-II	C	MF	8.82	84.5	18	0.532	0.636	0.868	0.872	0.827	0.890	0.810		0.858 ??
		HD-100	C	MF	13.18	85.0	18	0.529	0.636	0.868	0.872	0.827	0.890			0.870
Varley	19	Impeller 12	P	RF	9.60	88.0	5	0.338	0.195	0.672*	0.662	0.374	0.604		0.064	0.965*
Reddy	12	DM 1A	C	RF	27.36	90.0	14	***	0.558	0.842	0.836	0.776	0.859		0.363	0.809
		15 Bladed	C	RF	9.35	90.0	15	0.457	0.580	0.849	0.846	0.791	0.868	0.825		0.810
Balje	10	Auto GTC	C	RF	10.00	90.0	16	***	0.600	0.856	0.860	0.804	0.877			0.840
Dallenbach	20	Figure 36 (DVL)	C	MF		90.0	16	0.595	0.600	0.856	0.860	0.804	0.877	~.800	~.225	0.886
		Impeller B				90.0	17	***	0.618	0.862	0.865	0.815	0.884	0.874		
Wiesner	16	Figure 8 (NACA TN 1313)	C	RF	12.00	90.0	18	0.533	0.635	0.867	0.870	0.826	0.890		0.305	0.887
Wiesner	16	Figure 7	C	MF	15.40	90.0	19	0.461	0.650	0.872	0.875	0.835	0.896		0.350	0.882
Dallenbach	20	Impeller A	C	RF		90.0	19	***	0.650	0.872	0.875	0.835	0.896			
Stahler	24	19 Bladed	C	RF		90.0	19	***	0.650	0.872	0.875	0.835	0.896	0.870 (Per Eqn)		0.865
Stanitz	9	Radial Bladed	C	RF		90.0	20	0.490	0.664	0.877	0.880	0.843	0.901			
Campbell, Et al	5	Figure 8	C	MF	13.00	90.0	22	0.475	0.699	0.885	0.890	0.857	0.910	0.899		0.890
Sheets	7	Radial Bladed DC 8	C	RF	2.15	90.0	22	0.333	0.690	0.885	0.892	0.857	0.910	0.892	0.325	0.905
Sheets	6	Impeller B	C	RF	13.38	90.0	24	0.372	0.711	0.891	0.900	0.869	0.918			0.937
		R-303-1	C	RF	28.00	90.0	28	0.489	0.747	0.902	0.915	0.888	0.929		0.265	0.903
Ball, Et al	22	B.31	C	RF	6.83	90.0	30	0.497	0.761	0.907	0.920	0.895	0.934			0.916
						90.0	30	***	0.761	0.907	0.920	0.895	0.934			

* Includes Radius Ratio Correction & C_H Correction
** Per Wislicenus, for up to 16 blades, extrapolated beyond 16 blades
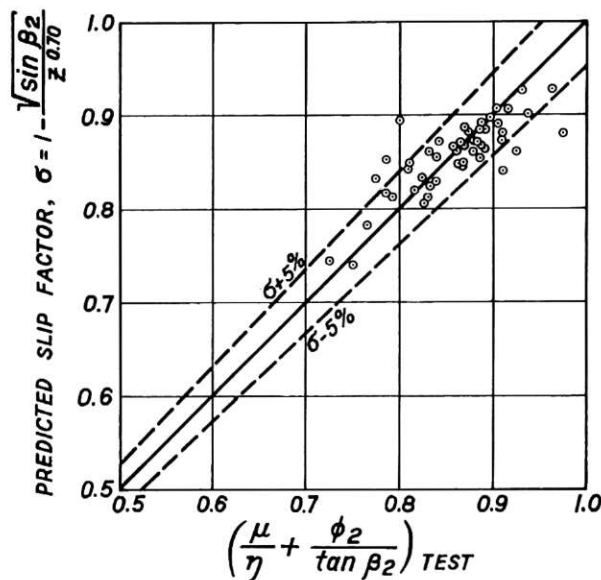*** Probably less than ε_{LIMIT}

Fig. 3 Correlation of empirical and test slip factors
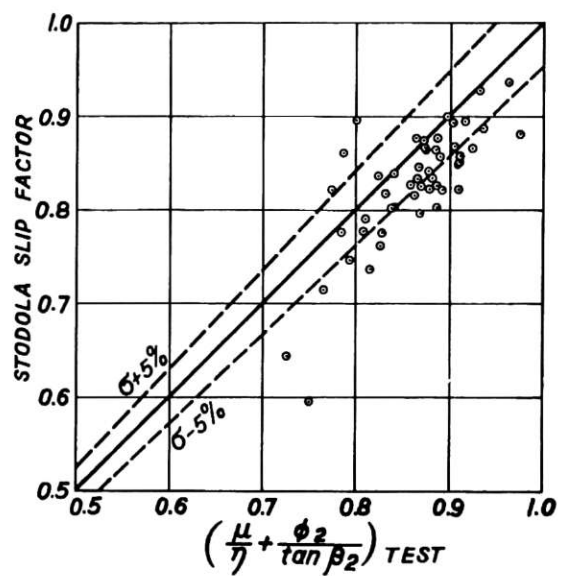

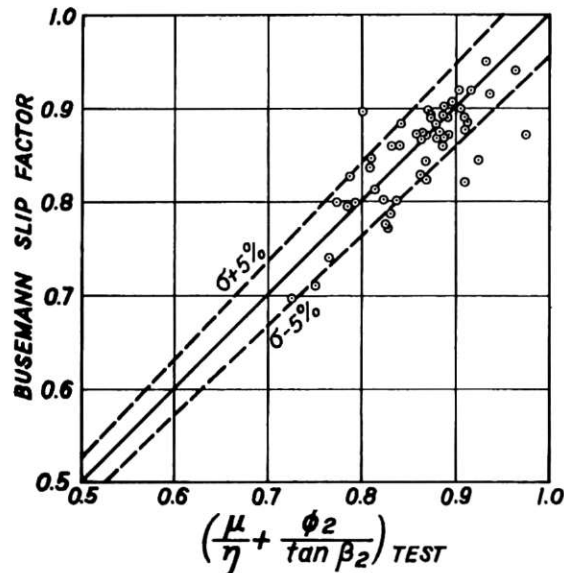Fig. 5 Correlation of Stodola and test slip factors

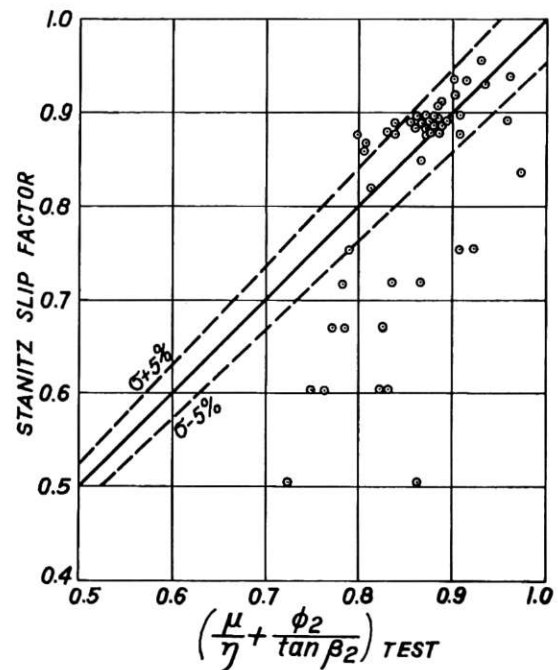Fig. 4 Correlation of Busemann and test slip factors

Fig. 6 Correlation of Stanitz and test slip factors

in Table 1 against slip factors obtained from equation (12) for all of the impellers which do not exceed their corresponding limiting radius ratios. This plot demonstrates that 46 of these stages (or about 88.5 percent) predict within ±5 percent of the corresponding test values. Plotting the Busemann slip factors in the same way, Fig. 4, indicates that 82.6 percent of these stages fall within the same band. Further, using the Stodola expression would show only 27 of these stages (or about 52 percent) within this band of "error," Fig. 5, and using the Stanitz equation, there would only be 30 stages (or about 57.6 percent) within this same band, Fig. 6.

The 13 stages for which the geometrical mean radius ratios were greater than the calculated mean radius ratio limits are plotted separately in Figs. 7 and 8. Fig. 7 shows that the predicted slip factors according to equation (14), for 7 of the 13 stages (about 54 percent) fall within ±5 percent of the corrected test results. Referring to Fig. 8, the Busemann slip factor does not seem to compare quite as well as this, with only 4 of the 13 stages (or about 31 percent) within the 5 percent error band.

In most cases, the Stodola and Stanitz slip factors for these stages would fall completely outside the 5 percent band, Table 1.

Certain series of tests, included in Table 1, have also been plotted separately in order to illustrate the degree of correlation which exists between the predicted slip factors from equations (12) or (14) and the corresponding test results. Fig. 9 shows these comparisons for Kearton's tests of 1933, and also indicates where the limiting radius ratio would occur for his particular series of 40-deg impellers. Fig. 10 depicts similar comparisons for Kasai's tests of 1935. Again, the location of the limiting radius ratio for his series of 7 bladed test impellers is also shown on this plot. Figs. 11 and 12 illustrate the slip factor correlations for both series of tests conducted by Varley in 1960 (27-deg impellers with varying number of blades, and 5 bladed impellers with varying discharge angles). Limiting radius ratios are also plotted on these charts.

Finally, Fig. 13 is included to demonstrate the comparison between the slip factors calculated using equations (12) or (14) and
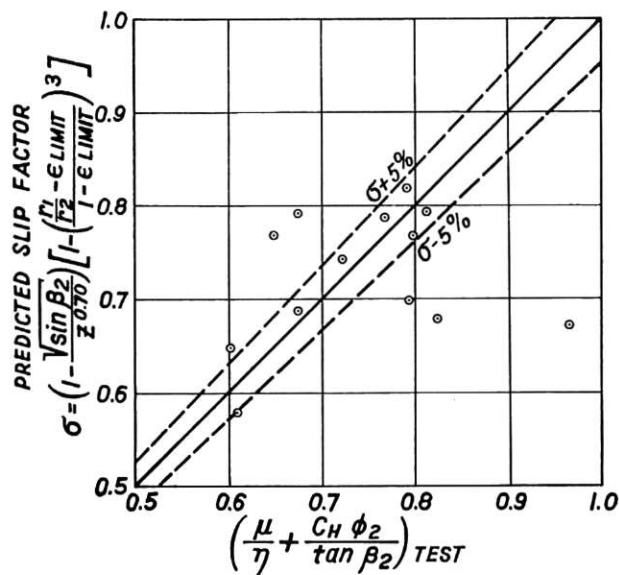
Fig. 7 Correlation of empirical and test slip factors for impellers having mean radius ratios greater than ϵ_{limit}
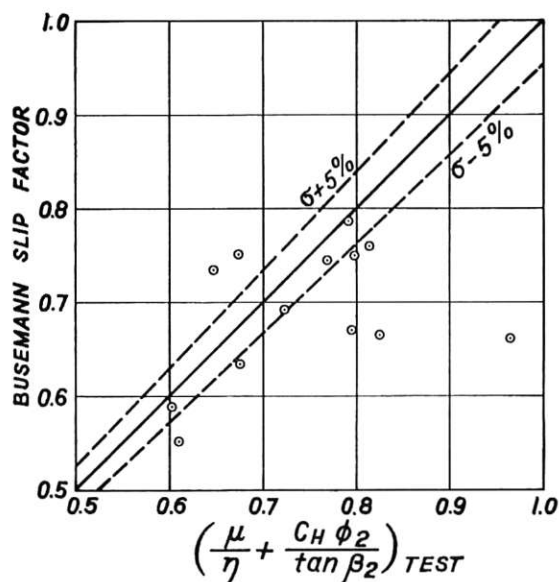

Fig. 9 Comparison of slip factors with Kearton's experimental results

Fig. 8 Correlation of Busemann and test slip factors for impellers having mean radius ratios greater than ϵ_{limit}

Fig. 10 Comparison of slip factors with Kasai's experimental results

those developed by Reddy [12], using his more extensive equation for radial bladed impellers. Also shown on this plot are the Stodola and Stanitz slip factors for radial bladed impellers, and a curve for the limiting radius ratios which are applicable to radial bladed impellers.

Conclusions

In consideration of all of the material presented in this review, it is concluded that the classical method proposed by Buseman is still the most generally applicable prediction for the basic slip factor of centrifugal impellers. It has been demonstrated that the simple empirical expression

$$\sigma = 1 - \frac{\sqrt{\sin \beta_2}}{Z^{0.70}}$$

fits the Busemann results extremely well over the whole range of practical blade angles and number of blades up to a limiting inlet to outlet mean radius ratio for the impeller
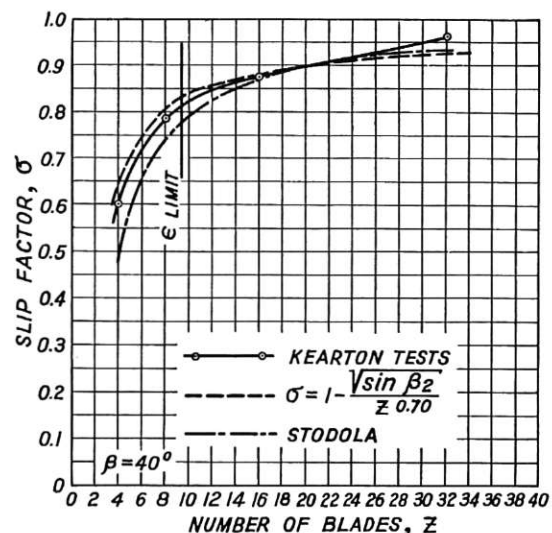

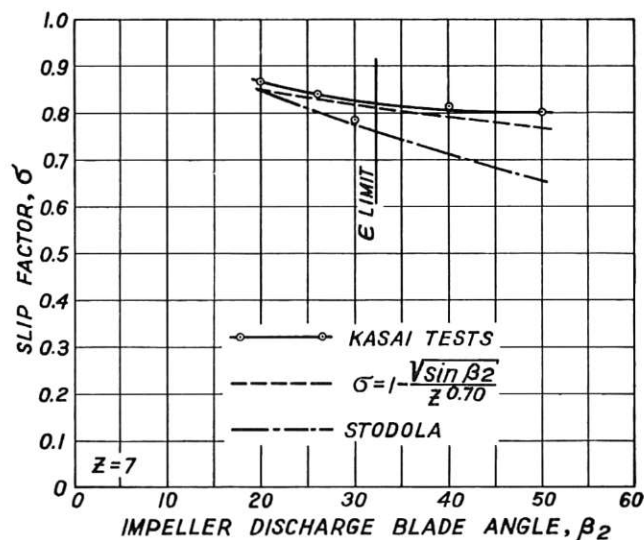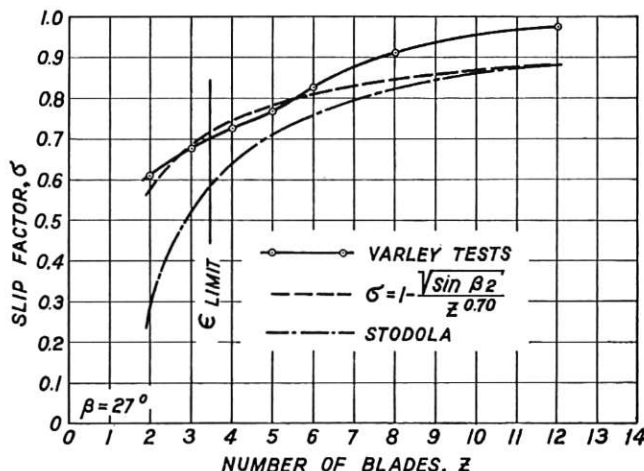**Fig. 11** Comparison of slip factors with Varley's experimental results (β_2 constant at 27 deg)
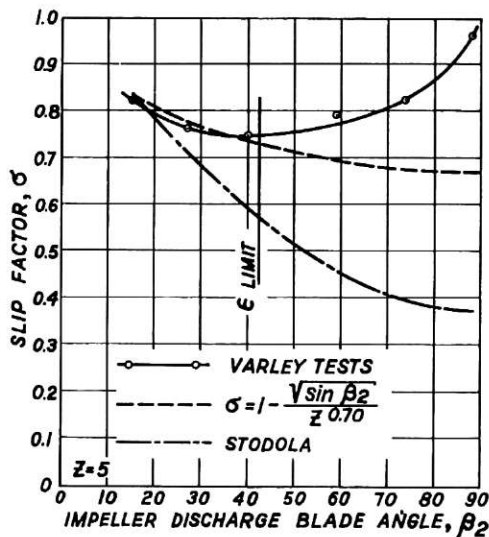
Fig. 12 Comparison of slip factors with Varley's experimental results (Z constant at 5 blades)

Fig. 13 Comparison of slip factors with some test results for radial bladed impellers

$$\epsilon_{\text{limit}} = \frac{r_1}{r_2} \cong \frac{1}{\ln^{-1}\dfrac{8.16 \sin \beta_2}{Z}}.$$

It is recommended that these relations be utilized for the fast and accurate determination of slip factors for all centrifugal impeller applications.

When the mean radius ratio of the impeller exceeds the limitation previously given, an empirical correction to the calculated slip factor according to the expression

$$\left[1 - \left(\frac{\dfrac{r_1}{r_2} - \epsilon_{\text{limit}}}{1 - \epsilon_{\text{limit}}} \right)^3 \right]$$

has been proposed. Although the resulting slip factors calculated for this region of application appear to be in fair agreement with those of Busemann, and there would seem to be an even better agreement between these equations and the experimental results (compare Figs. 7 and 8), further work must be accomplished in this area before a firm recommendation can be made to employ this particular slip correction factor.

Acknowledgments

The author wishes to express his appreciation to Carrier Air Conditioning Company for permission to publish this paper and to include certain of the test information contained herein. Thanks are also given to Mr. Richard E. Filippi, for his technical assistance during the preparation of the manuscript, and to Mr. Herbert N. Sturms, for his excellent work in preparing the various diagrams.

References

1 A. Stodola, *Steam and Gas Turbines*, McGraw-Hill Book Company, New York, N. Y., 1927.

2 A. Busemann, "Das Forderhohenverhaltniss radialer Kreiselpumpen mit logarithmischspiraligen Schaufeln," *Zeitschrift für Angewandte Mathematik und Mechanik*, vol. 8, October, 1928, pp. 372–384.

3 W. F. Kearton, "The Influence of the Number of Impeller Blades on the Pressure Generated in a Centrifugal Compressor and on Its General Performance," *Proceedings, Institution of Mechanical Engineers*, London, vol. 124, 1933, p. 481.

4 T. Kasai, "On the Exit Velocity and Slip Coefficient of Flow at the Outlet of the Centrifugal Pump Impeller," *Memoirs of the Faculty of Engineering*, Kyushu Imperial University, Japan, vol. 8, no. 1, 1936.

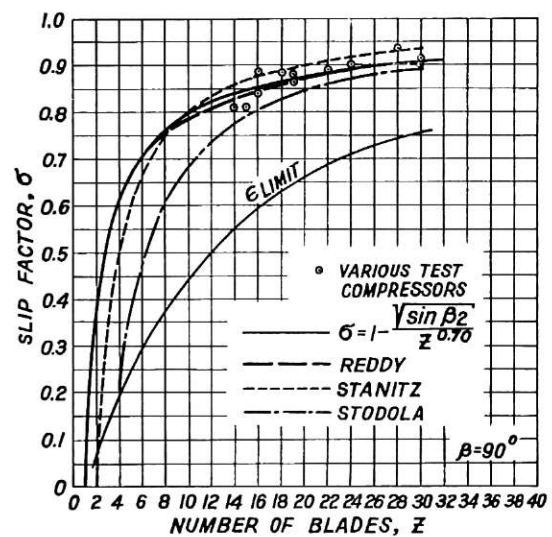5 K. Campbell and J. E. Talbert, "Some Advantages and Limita-tions of Centrifugal and Axial Aircraft Compressors," *SAE Transactions*, vol. 53, no. 10, October, 1945, p. 607.

6 G. F. Wislicenus, *Fluid Mechanics of Turbomachinery*, Mc-Graw-Hill Book Company, New York, N. Y., 1947.

7 H. E. Sheets, "The Flow Through Centrifugal Compressors and Pumps," TRANS. ASME, vol. 72, 1950, pp. 1009–1015.

8 J. F. Peck, "Investigation Concerning Flow Conditions in a Centrifugal Pump and the Effect of Blade Loading on Head Slip," *Proceedings, Institution of Mechanical Engineers*, London, vol. 164, no. 1, 1951, p. 1 (including discussions by Hutton and Worster).

9 J. D. Stanitz, "Some Theoretical Aerodynamic Investigations of Impellers in Radial and Mixed-Flow Centrifugal Compressors," TRANS. ASME, vol. 74, 1952, pp. 473–497.

10 O. E. Balje, "A Contribution to the Problem of Designing Radial Turbomachines," TRANS. ASME, vol. 74, 1952, pp. 451–472.

11 L. R. Wosika, "Radial-Flow Compressors and Turbines for the Simple Small Gas Turbine," TRANS. ASME, vol. 74, 1952, pp. 1337–1347.

12 K. R. Reddy, "Relative Eddy and Its Effects on the Performance of a Radial Bladed Centrifugal Impeller," *Journal of the Royal Aeronautical Society, London*, August, 1954, p. 547.

13 D. G. Shepherd, *Principles of Turbomachines*, The Macmillan Company, New York, N. Y., 1956.

14 A. J. Acosta and R. D. Bowerman, "An Experimental Study of Centrifugal-Pump Impellers," TRANS. ASME, vol. 79, 1957, pp. 1821–1839.

15 G. Kamimoto and Y. Matsuoka, "Theory of Centrifugal-Type Impeller With Vanes of Arbitrary Form," *Bulletin Japan Society of Mechanical Engineers*, vol. 2, no. 8, 1959, p. 630.

16 F. J. Wiesner, "Practical Stage Performance Correlations for Centrifugal Compressors," ASME Paper No. 60-Hyd-17.

17 J. J. Kramer, W. M. Osborn, and J. T. Hamrick, "Design and Test of Mixed-Flow and Centrifugal Impellers," JOURNAL OF ENGINEERING FOR POWER, TRANS. ASME, Series A, vol. 82, 1960, pp. 127–135.

18 G. T. Csanady, "Head Correction Factors for Radial Impellers," *Engineering*, London, vol. 190, 1960, p. 195.

19 F. A. Varley, "Effects of Impeller Design and Surface Roughness on the Performance of Centrifugal Pumps," *Proceedings, Institution of Mechanical Engineers*, London, vol. 175, 1961.

20 F. Dallenbach, "The Aerodynamic Design and Performance of Centrifugal and Mixed-Flow Compressors," *Centrifugal Compressors*, SAE Technical Progress Series, vol. 3, 1961.

21 C. Rodgers, "Influence of Impeller and Diffuser Characteristics and Matching on Radial Compressor Performance," *Centrifugal Compressors*, SAE Technical Progress Series, vol. 3, 1961.

22 G. A. Ball, A. H. Bell, and L. B. Mann, "The Development of the Chrysler Automotive Centrifugal Compressor," *Centrifugal Compressors*, SAE Technical Progress Series, vol. 3, 1961.

23 T. B. Ferguson, *The Centrifugal Compressor Stage*, Butterworth & Company, London, 1963.

24 Alfred E. Stahler, "The Slip Factor of a Radial Bladed Centrifugal Compressor," ASME Paper No. 64—GTP-1.

25 G. M. Wood, H. Welna, and R. P. Lamers, "Tip-Clearance Effects in Centrifugal Pumps," *Journal of Basic Engineering*, TRANS. ASME, Series D, vol. 87, 1965, pp. 932–940.